Chemical Engineering Journal 96 (2003) 29–35

Chemical Engineering Journal

www.elsevier.com/locate/cej

# Gas–liquid mass transfer in slurry bubble systems II. Verification and simulation of the model based on the single bubble mechanism

Weiguo Yang, Jinfu Wang*, Bin Zhao, Yong Jin

*Department of Chemical Engineering, Tsinghua University, Beijing 100084, PR China*

**Abstract**

Bubble sizes, interfacial areas and volumetric mass transfer coefficients in a slurry bubble column are measured experimentally and used to determine the two parameters of a mass transfer model. The mass transfer coefficients $k_L$ between the gas and liquid phases in a slurry bubble column under different operating conditions are simulated. Calculated results show very good agreement with experimental measurements. The mass transfer model proposed can predict well the mass transfer rate in slurry bubble systems.


*Keywords:* Slurry bubble column; Gas–liquid mass transfer; Mathematical model; Interfacial area

## 1. Introduction

Gas–liquid mass transfer is an important process in a number of chemical engineering unit operations such as gas–liquid and gas–liquid–solid reaction, distillation and absorption. It is a common problem to predict the mass transfer rate in a variety of chemical synthesis, petrochemical manufacturing, energy transformation, environmental engineering and biochemical engineering. Thus, it is necessary to have a better understanding of the mechanism and characteristics of gas–liquid mass transfer. Researches on the relationship, interactions and influences of chemical reaction and mass transfer are also significant for developing efficient gas–liquid mass transfer and for the optimal design of novel commercial gas–liquid–solid three-phase reactors [1].

Researches on interfacial mass transfer has been continuously carried out since Lewis and Whitman proposed the two-film theory for interfacial mass transfer in 1923 [2]. The film penetration model [3], surface renewal model [4] and unsteady state two-film model [5,6] were developed in succession through efforts made to establish mass transfer models with wider applicability and higher precision in prediction. However, mass transfer models suitable for slurry bubble systems are still scarce in the literature of chemical engineering.

A slurry bubble system is a complicated reaction system because it consists of different gases, liquids and particles. The slurry bubble system used in this paper is a typical and practical system with CO and $H_2$ as the gas phase, paraffin as the liquid-phase and catalysis powder as the solid phase. This system is important due to its application in Fischer–Tropsch synthesis, and the liquid-phase methanol and dimethylether (DME) synthesis processes. Some research work on this system has been carried out in recent years and the influence of the pressure [7–9], temperature [7,10] and superficial gas velocity [11] on mass transfer has been reported in the literature. However, the results reported in the literature were not coherent and were even contradictory [7,10], and there is a lack of suitable mathematical model that simulates interfacial mass transfer in slurry bubble systems.

A new macroscopic model for gas–liquid interfacial mass transfer in slurry bubble systems was established in the first part of this work. It is based on the unsteady state film mass transfer mechanism. An analytical solution of the model was obtained by Laplace transformation and statistical integration. The influence of the model parameters on the interfacial mass transfer rate was determined by numerical simulation.

Bubble sizes and their distribution, gas–liquid interfacial areas and the volumetric interfacial mass transfer coefficients $k_La$ measured experimentally are reported in this paper. The mass transfer coefficient $k_L$ can be calculated from the measured gas–liquid interface area and volumetric

* Corresponding author. Tel.: +86-10-62785464; fax: +86-10-62772051.
*E-mail address:* wangjf@flotu.org (J. Wang).

1385-8947/$ – see front matter © 2003 Elsevier B.V. All rights reserved.
doi:10.1016/j.cej.2003.08.013

**Nomenclature**

| | |
|---|---|
| $a$ | specific gas–liquid interfacial area ($m^{-1}$) |
| $C_A$ | microcosmic gas concentration in liquid-phase ($mol\,l^{-1}$) |
| $C_A^*$ | saturated gas concentration in liquid-phase ($mol\,l^{-1}$) |
| $C_v$ | volume percentage of solid in slurry |
| $Eu$ | Euler number ($=P/\rho_{SL}U_G^2$) |
| $k_L$ | gas–liquid mass transfer coefficient ($m\,s^{-1}$) |
| $k_La$ | gas–liquid volumetric mass transfer coefficient ($s^{-1}$) |
| $N$ | molar flow rate ($mol\,s^{-1}$) |
| $P$ | gauge pressure (MPa) |
| $R$ | radius of bubble (m) |
| $Re$ | Reynolds number ($=d\rho_{SL}U_G/\mu_{SL}$) |
| $s$ | surface renewal constant ($s^{-1}$) |
| $Sc$ | Schmidt number ($=\mu_{SL}/\rho_{SL}D_A$) |
| $t$ | time (s) |
| $T$ | temperature (K) |
| $U_g$ | superficial gas velocity ($m\,s^{-1}$) |
| $V$ | volume ($m^3$) |

*Greek symbols*

| | |
|---|---|
| $\delta$ | thickness of the mass transfer liquid film (m) |
| $\mu_{SL}$ | superficial viscosity of the slurry (Pa s) |
| $\rho_{SL}$ | superficial density of the slurry ($kg\,m^{-3}$) |

interfacial mass transfer coefficient $k_La$. The two parameters in the mass transfer model developed in the first part of this work are determined from the experimental measurements, and are correlated with the system properties and the operating conditions of the slurry bubble column including the pressure, temperature, superficial gas velocity and particle concentration. The gas–liquid mass transfer coefficient $k_L$ under different operating conditions are simulated by the mathematical model. The measured and calculated values of the gas–liquid mass transfer coefficient $k_L$ are compared and good agreement between the experimental and simulated results is obtained. This semi-theoretical model can predict the gas–liquid mass transfer coefficient $k_L$ and the volumetric mass transfer rate in slurry bubble reactors with satisfactory precision.

## 2. Experimental

Fig. 1 shows the experimental apparatus used to investigate mass transfer in the slurry bubble column. The experimental setup consists of a reactor of ∅ 37 mm in i.d. and 480 mm in height, a pipeline system with two triple valves and a sampling system. The temperature and pressure ranges adopted in the experiments are from room temperature to 300 °C and from atmospheric pressure to 6 MPa which are in the range of operating conditions used in industrial practice. The liquid-phase used is liquid paraffin. The solid particle is silica gel powder with a mean diameter of 134 μm. The gas phase is $N_2$, CO and $H_2$. In the experiments, gas flows from steel cylinders into the reactor entrance through

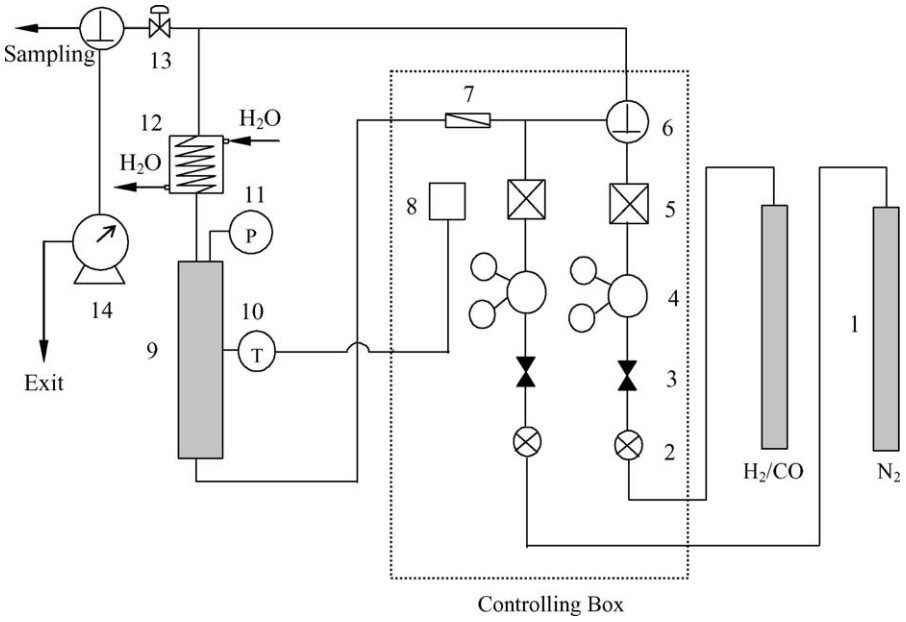


Fig. 1. Experimental set-up: (1) cylinder; (2) filter; (3) shutoff valve; (4) reducing pressure regulator; (5) mass flow controller; (6) triple valve; (7) check valve; (8) temperature controller; (9) reactor; (10) thermocouple; (11) pressure gauge; (12) condenser; (13) back pressure regulator; (14) wet flow meter.

the gas filter, shutoff valve and pressure reducing regulator, successively. The pressure reducing regulator is used to adjust the entrance pressure of the reactor. The gas flow-rate is measured and controlled by a mass flow controller. The temperature in the reactor is measured by thermocouples and controlled by a temperature controller. The pressure in the reactor is adjusted by a back pressure regulator at the outlet and the outlet gas is vented through a triple valve and a wet gas flow meter.

The volumetric mass transfer coefficients $k_L a$ of $H_2$ and CO are determined by measuring their gas absorption rate into the slurry phase [12]. The composition of the exit gas is analyzed online by gas chromatography to determine the concentration of absorbed gases in the slurry phase.

The experiments are carried out under different temperatures, pressures and inlet gas concentrations. Before measuring the gas absorption, $N_2$ as an inert gas is introduced into the reactor to strip off $H_2$ and CO from the slurry phase. In the experiments, gas A, $H_2$ or CO, is fed into the reactor at a fixed volumetric flow-rate $N_{A0}$ beginning from $t_0 = 0$. At time $t = t_i$ ($i = 1, 2, \ldots, n$) at equal intervals, the outlet gas is sampled and analyzed by gas chromatography after the pressure is reduced. The flow-rate of the outlet gas $N_O(t_i)$ is also recorded until the gas in the slurry phase is saturated at time $t = t_n$. The instantaneous concentration of gas A in the slurry phase $C_A(t_i)$ can be obtained by

$$C_A(t_i) = \frac{1}{V_L}\left[N_{A0}t_i - \int_0^{t_i} N_O(t_i)x_A(t_i)\,dt\right] \quad (1)$$

where $N_{A0}$ is the flow-rate of inlet gas A and $V_L$ the volume of the slurry phase. The integral term in Eq. (1) can be calculated by the trapezoid formula

$$\int_0^{t_i} N_O(t_i)x_A(t_i)\,dt = \sum_1^i \frac{1}{2}\left[N_O(t_i)x_A(t_i) + N_O(t_{i-1})x_A(t_{i-1})\right](t_i - t_{i-1}) \quad (2)$$

According to the mass conservation principle, the overall mass transfer rate $N_A A$ is determined by

$$N_A A = \frac{d[C_A(t)V_L]}{dt} = k_L A[C_A^* - C_A(t)] \quad (3)$$

or

$$\frac{dC_A(t)}{dt} = k_L a[C_A^* - C_A(t)] \quad (4)$$

where $a = A/V_L$ is the specific interfacial area and $C_A^* = C_A(t_n)$ is the equilibrium concentration of absorbed gas A in the slurry phase. The integral of Eq. (5) yields

$$-\ln\left[1 - \frac{C_A(t)}{C_A^*}\right] = k_L a t \quad (5)$$

Using the above equation and the measured concentrations, $k_L a$ can be obtained by determining the slope of the curve of $-\ln(1 - C_A(t)/C_A^*)$ versus time $t$ [11].

Bubble sizes and their distribution as well as the bubble rise velocity are measured experimentally using a fiber optic probe. The measuring principle is based on the difference in the reflection of light in the gas and liquid [13]. The intensity of the reflected signals is low when the probe is

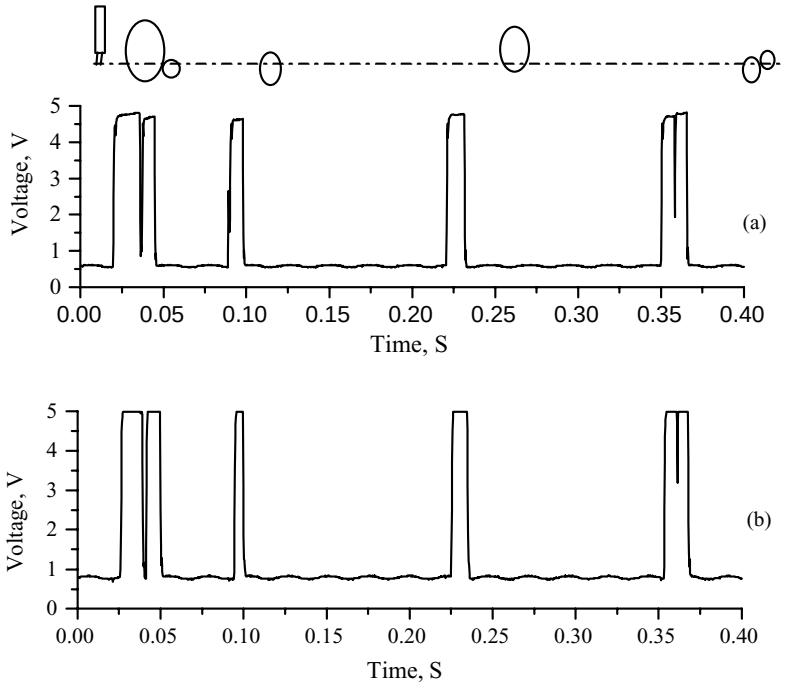


Fig. 2. Typical signals obtained by the fiber optic probe.

in the liquid-phase, and is high when it is in a bubble. As the gas slurry mixture flows up concurrently, output signals containing bubble information are obtained, as shown in Fig. 2. The downstream signals (b) lag a little compared with the upstream signals (a) due to the distance between the two fiber optic probes.

By processing the signals collected by the fiber optic probes, properties of the bubbles like bubble sizes and their distribution, rise velocity of the bubbles and gas hold-up can be obtained. The Sauter average diameter $d_{32}$, viz. the average diameter related to the volumetric surface, can be statistically calculated [13] from the plentiful bubble signals. With the Sauter average diameter of the whole system and the measured gas hold-up, the contact area of the gas–liquid interface can be obtained. Hence, the volumetric mass transfer coefficient $k_L a$ can be separated into a liquid film mass transfer coefficient $k_L$ and a specific interface $a$.

## 3. Determination of model parameters $s$ and $\delta$

The two model parameters $s$ and $\delta$ are determined using the Marquardt method for nonlinear parameter estimation. The initial values of $s$ and $\delta$ at the given operating conditions are first assumed, then calculated $k_L$ values are compared with experimental values [11]. The calculation is repeated until the iteration reaches a specified precision. The numerical calculation procedure is illustrated in Fig. 3.

In order to use the mass transfer model developed in the first part to predict the mass transfer rate under different conditions, the two model parameters are correlated with the operating conditions based on the experimentally measured results. Two sets of model parameters were obtained corresponding to $H_2$ and CO, respectively, as follows:

$$\delta_{H_2} = 6.706 \times 10^{-3} Eu^{-0.163} Re^{0.262} Sc^{0.779} C_v^{1.250} \quad (6)$$

$$s_{H_2} = 2.835 Eu^{0.065} Re^{0.231} Sc^{-0.618} C_v^{-0.089} \quad (7)$$

$$\delta_{CO} = 1.536 \times 10^{-6} Eu^{0.206} Re^{0.067} Sc^{0.165} C_v^{0.033} \quad (8)$$

$$s_{CO} = 7.401 \times 10^{-3} Eu^{0.422} Re^{0.341} Sc^{-0.340} C_v^{0.094} \quad (9)$$

The above correlation are valid in value ranges of the mentioned experimental conditions which correspond to $3.6 \times 10^6 < Eu < 1.5 \times 10^8$, $8 < Re < 340$, $13 < Sc < 360$ and $0 < C_v < 25$ vol.%. The gas–liquid mass transfer coefficient $k_L$ can be calculated under any given operating conditions from the above correlation. That is, the mass transfer model has prediction capability.

## 4. Analysis and discussion

Figs. 4–7 show the comparisons of the calculated and experimental $k_L$ values for $H_2$ and CO under different operating conditions. It can be seen that the calculated results agree very well with the experimental results. All these comparisons indicate the validity of the mass transfer model developed in this work. The abundant experimental measurements also ensure the applicability and accuracy of the model for the prediction of mass transfer in slurry bubble systems.

### 4.1. The influence of pressure

Fig. 4 shows the influence of pressure on the mass transfer coefficient $k_L$ into the slurry phase consisting of liquid paraffin and silica gel powder. The mass transfer coefficients of $H_2$ and CO into the slurry phase are presented in Fig. 4(a) and (b), respectively. It can be seen that the influence of pressure is not prominent in the experimental condition. It is not difficult to understand these results by considering the influence of pressure on the bubble size, bubble rise velocity and liquid film characteristics simultaneously. Pressure affects interface renewal slightly, but a high pressure leads to a decrease in the bubble size. Then it results in a decrease of bubble rise velocity and an increase in the liquid film thickness, which causes a slight decrease in the mass transfer coefficient $k_L$. However, increasing temperature weakens this trend and even increases the mass transfer coefficient $k_L$ of $H_2$ at higher temperatures. The reason is that an increase in temperature intensifies gas molecule movement and surface renewal, which enhances mass transfer.

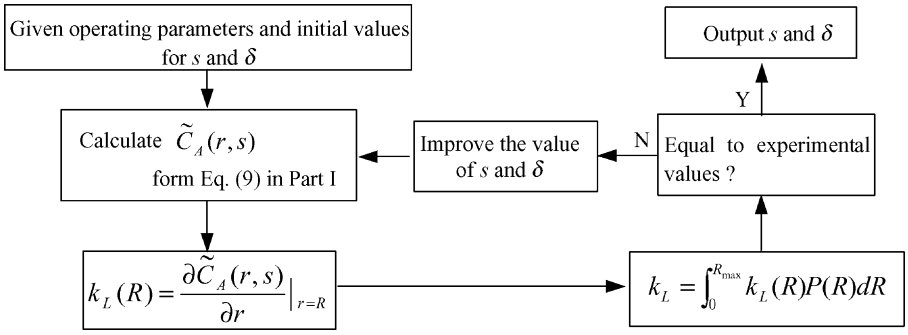


Fig. 3. Flow diagram for the determination of $s$ and $\delta$.

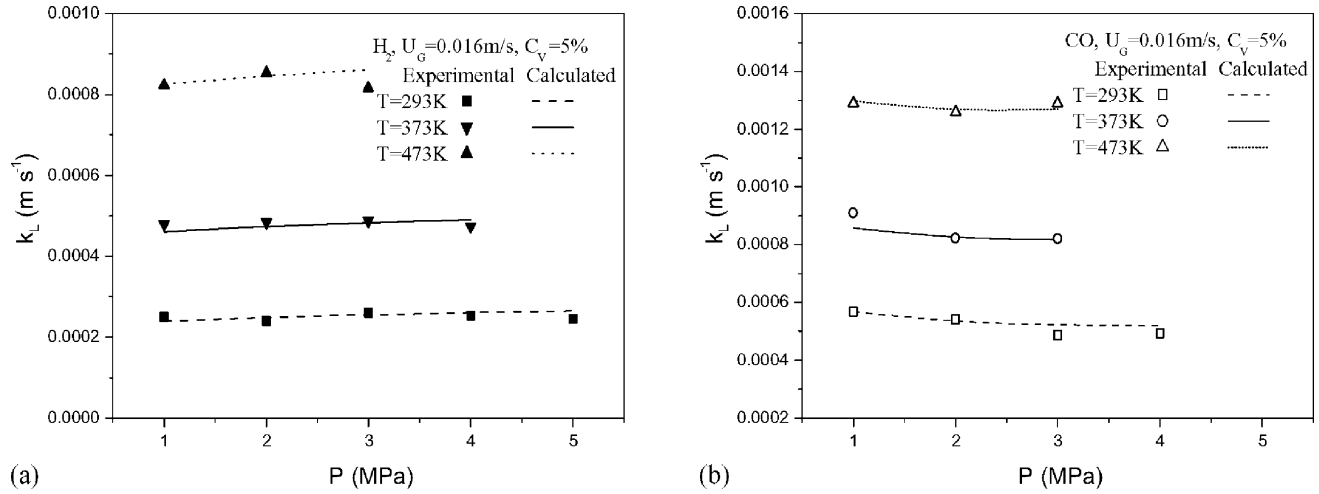


Fig. 4. Comparison of predicted and experimental $k_L$ values under different pressures: (a) for $H_2$; (b) for CO.

### 4.2. The influence of temperature

Fig. 5(a) and (b) shows the influence of temperature on the mass transfer coefficients $k_L$ of $H_2$ and CO into the liquid paraffin, respectively. It can be seen that the mass transfer coefficient $k_L$ values increase with temperature remarkably. The temperature influences both the thickness of the mass transfer liquid film $\delta$ and the surface renewal rate $s$. On the one hand, increasing temperature intensifies bubble coalescence, which leads to a larger size and faster movement of the bubbles. This will result in a decrease of the thickness of the mass transfer liquid film $\delta$, and the mass transfer coefficient $k_L$ increases. On the other hand, a high temperature favors the diffusion of gas molecules in the liquid film, which also results in an increase of the mass transfer coefficient $k_L$.

### 4.3. The influence of the superficial gas velocity

Fig. 6(a) and (b) present the influence of the superficial gas velocity on the mass transfer coefficients $k_L$ of $H_2$ and CO in the slurry bubble column, respectively. Similar to the influence of pressure, the influence of the superficial gas velocity is also not distinct. The bubble rise velocity increases and the thickness of the liquid film decreases with an increase of the superficial gas velocity. In addition, the increase of superficial gas velocity reduces the bubble residence time and leads to a decrease of the bubble surface renewal rate $s$. Therefore, both effects results in a small influence of the superficial gas velocity on the mass transfer coefficient $k_L$.

### 4.4. The influence of solid concentration

Fig. 7(a) and (b) shows the influence of solid concentration on the mass transfer coefficients $k_L$ of $H_2$ and CO, respectively. It can be seen that a high solid concentration in the slurry phase affects the mass transfer coefficients $k_L$ of both $H_2$ and CO into the slurry phase unfavorably. The values of mass transfer coefficients $k_L$ decrease slightly with an increase in the solid concentration.

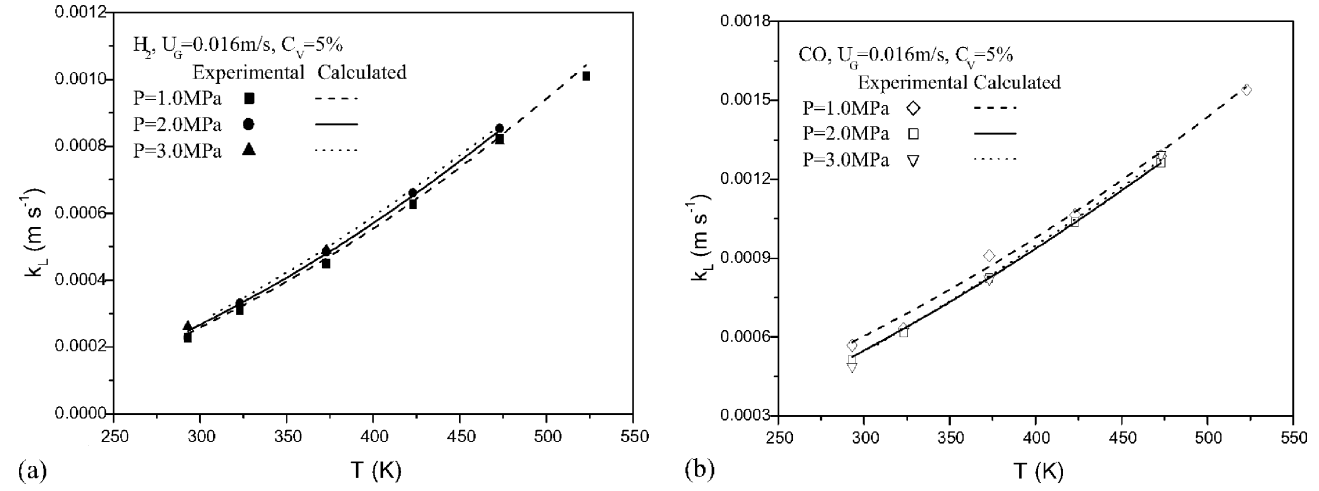


Fig. 5. Comparison of predicted and experimental $k_L$ values at different temperatures: (a) for $H_2$; (b) for CO.

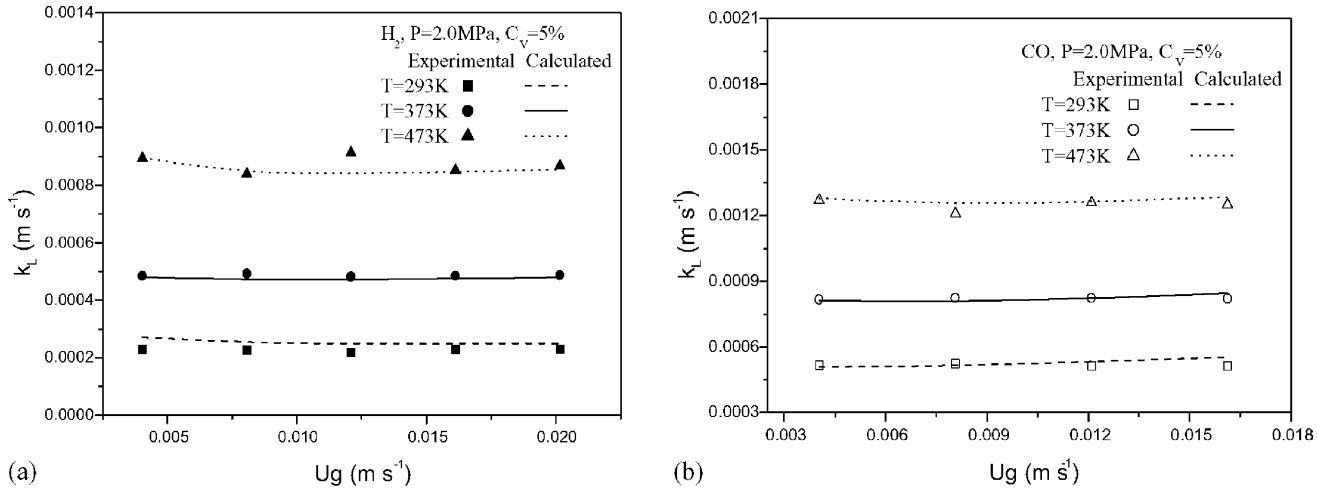


Fig. 6. Influence of superficial gas velocities on the mass transfer coefficients $k_L$: (a) for $H_2$; (b) for CO.

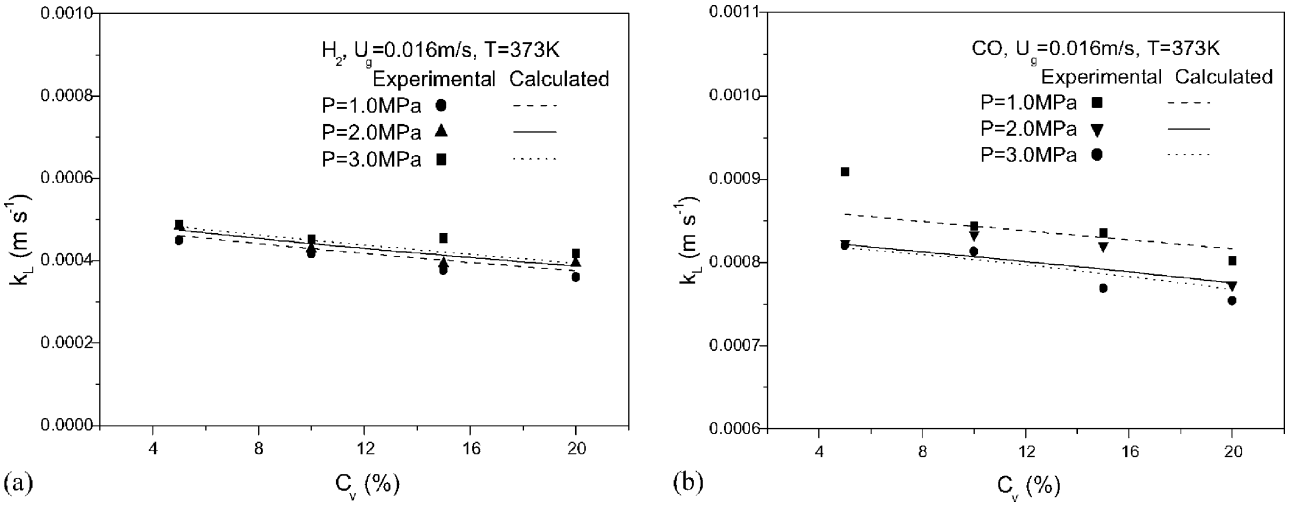


Fig. 7. Influence of solid concentrations on the mass transfer coefficients $k_L$: (a) for $H_2$; (b) for CO.

It is known that the system superficial viscosity increases with an increase in the solid concentration. High system viscosity weakens the turbulence in the system and decreases the bubble rise velocity. The system viscosity also affects the surface renewal rate *s*. Although a high solid concentration can lead to the formation of larger bubbles, the influence of the system viscosity dominates the mass transfer in this case and the mass transfer coefficient $k_L$ decreases as the solid concentration increases.

## 5. Conclusions

A mass transfer model with two parameters with explicit physical meanings is established for slurry bubble systems which is based on the unsteady state film mass transfer mechanism to a single bubble. The two model parameters are correlated with the operating conditions using experimental results. The influences of different operating factors on the mass transfer coefficient are simulated using different operating conditions. Calculated results from the model agree with the experimental measurements well for all the experimental conditions which indicate the validity and applicability of the mass transfer model. The new model can be used to predict the mass transfer rate in slurry bubble systems and is useful for the design and optimum operation of slurry bubble column reactors.

## Acknowledgements

The authors gratefully acknowledge the financial support by the Chinese National Science Foundation (No. 20276035) and by the Sinopec Fundamental Research Foundation (No. X500021).

## References

[1] F.S. Fan, Gas–Liquid–Solid Fluidization Engineering, Butterworths, Boston, 1989.
[2] W.K. Lewis, W.G. Whitman, Principles of gas absorption, Ind. Eng. Chem. 16 (1924) 1215–1220.
[3] H.L. Toor, J.M. Marchello, Film-penetration model for mass and heat transfer, AIChE J. 4 (1958) 97–101.
[4] P.V. Danckwerts, Significance of liquid-film coefficients in gas absorption, Ind. Eng. Chem. 43 (1951) 1460–1467.
[5] J.F. Wang, H. Langemann, Unsteady two-film model for mass transfer, Chem. Eng. Technol. 17 (1994) 280–284.
[6] J.F. Wang, H. Langemann, Unsteady two-film model for mass transfer accompanied by chemical reaction, Chem. Eng. Sci. 49 (1994) 3457–3463.
[7] M.-Y. Chang, J.G. Eiras, B.I. Morsi, Mass transfer characteristics of gases in *n*-hexane at elevated pressures and temperatures in agitated reactors, Chem. Eng. Process. 29 (1991) 49–60.
[8] M.-Y. Chang, B.I. Morsi, Mass transfer characteristics of gases in aqueous and organic liquids at elevated pressures and temperatures in agitated reactors, Chem. Eng. Sci. 46 (1991) 2639–2650.
[9] M. Teramoto, S. Tai, K. Nishii, H. Teranishi, Effects of pressure on liquid-phase mass transfer coefficients, Chem. Eng. J. 8 (1974) 223–226.
[10] B.M. Karandikar, B.I. Morsi, Y.T. Shah, Effect of water on the solubility and mass transfer coefficients of CO and $H_2$ in a Fischer–Tropsch liquid, Chem. Eng. J. 33 (1986) 157–168.
[11] W.G. Yang, J.F. Wang, Y. Jin, Mass transfer of syngas components in slurry system at industrial conditions, Chem. Eng. Technol. 24 (2001) 651–657.
[12] W.G. Yang, J.F. Wang, Y. Jin, Mass transfer behavior in high temperature and high pressure slurry bubble columns, in: Proceedings of the Seventh China–Japan Symposium on Fluidization, 2000, pp. 190–195.
[13] T.F. Wang, J.F. Wang, W.G. Yang, Y. Jin, Bubble behavior in gas–liquid–solid three-phase circulating fluidized beds, Chem. Eng. J. 38 (2001) 397–404.